

The partially disordered state of the frustrated face-centred cubic antiferromagnet GdInCu_4

This article has been downloaded from IOPscience. Please scroll down to see the full text article.

1999 *J. Phys.: Condens. Matter* 11 1095

(<http://iopscience.iop.org/0953-8984/11/4/017>)

[View the table of contents for this issue](#), or go to the [journal homepage](#) for more

Download details:

IP Address: 130.209.6.50

The article was downloaded on 12/06/2013 at 03:23

Please note that [terms and conditions apply](#).

The partially disordered state of the frustrated face-centred cubic antiferromagnet GdInCu_4

H Nakamura[†], N Kim[†], M Shiga[†], R Kmiec[‡], K Tomala[§], E Ressouche^{||},
J P Sanchez^{||} and B Malaman[¶]

[†] Department of Materials Science and Engineering, Kyoto University, Kyoto 606-8501, Japan

[‡] H Niewodniczanski Institute of Nuclear Physics, Cracow, Poland

[§] Institute of Physics, Jagellonian University, Cracow, Poland

^{||} Département de Recherche Fondamentale sur la Matière Condensée, SPSMS, CEA-Grenoble, 38054 Grenoble Cédex 9, France

[¶] Laboratoire de Chimie du Solide Minéral Associé au CNRS, Université Henri Poincaré, Nancy I, BP239, 54506 Vandoeuvre les Nancy Cedex, France

Received 7 October 1998

Abstract. The magnetic structure of the frustrated fcc antiferromagnet GdInCu_4 was investigated by measuring the magnetic susceptibility, ^{155}Gd Mössbauer effect and neutron diffraction. We propose a partially disordered structure of type III ($Q = (0\frac{1}{2}1)$), in which only the Gd atoms in every second (010) layer are ordered and the remaining half of the atoms sandwiched by the static layers fluctuate dynamically just below T_N and slow down to exhibit glass-like freezing of the layers at lower temperatures. This partially disordered state is the first example found for the fcc lattice which is driven not by the moment instability but by the dynamical (entropy) effect.

1. Introduction

The effects of geometrical frustration on magnetism are currently attracting considerable attention, since they often lead to exotic quantum states [1]. Although the frustration of anti-ferromagnetic interactions has been extensively investigated for low-dimensional systems, it is also well known that all Ising, XY and Heisenberg spins frustrate on a regular tetrahedron. A face-centred cubic (fcc) lattice is the simplest example of an infinite network of tetrahedra. Although theoretical studies of the ground state of the nearest-neighbour antiferromagnetic Ising spins on the fcc lattice, initiated by Anderson [2], have a long history, even this simplest problem has not been solved exactly, and still attracts theoretical interest. In contrast, the experimental situations are rather simple. Most of the fcc compounds (except some Kondo and itinerant-electron systems) exhibit well-defined magnetic ordering, and their propagation vectors, Q , are classified into a few categories. These structure types are usually interpreted in terms of molecular-field theory taking into account nearest-neighbour (nn) and next-nearest-neighbour (nnn) interactions J_1 and J_2 [3]. This is based on close nn and nnn distances in the fcc lattice. Therefore, the geometrical frustration on the nn fcc antiferromagnet seems to be an issue only as regards theory.

GdInCu_4 may represent a suitable experimental subject for a study of such matters, since this is a unique fcc antiferromagnet with dominant interactions $J_1 (<0)$ [4–6]. The crystal structure is of the cubic C15b type, in which well-localized Gd spins with no orbital moment form an fcc lattice. GdInCu_4 exhibits an antiferromagnetic transition at a very low temperature

of $T_N \simeq 7$ K, despite the strong antiferromagnetic interactions expected from the paramagnetic Curie temperature, $\theta_p \simeq -45$ K. The ratio $|\theta_p|/T_N$ is the largest among the conductive Gd compounds. The magnetic entropy reaches only about 60% of the expected value just above T_N , indicating that short-range magnetic correlations persist above T_N . These features point to strong effects of the frustration. Furthermore, GdInCu₄ is a low-carrier-density (semimetallic) system, implying that short-range superexchange interactions, probably via In atoms, are dominant. Thus, it is of interest to study the ground state of GdInCu₄ as a low-carrier-density frustrated fcc antiferromagnet with $|J_1| \gg |J_2|$. Recently, a three-dimensional network of corner-sharing tetrahedra, such as is found in pyrochlore, spinel and Laves phases, has attracted considerable attention. For this lattice, a nonmagnetic (spin-singlet-like) ground state has been suggested on the basis of some theories [7], and a spin-liquid-like behaviour was actually found experimentally [8]. In addition, in the fcc lattice, since it seems that degeneracies are not sufficient for realizing a nonmagnetic ground state [9], a certain unconventional magnetic ordering is expected.

In order to identify the low-temperature magnetic state of GdInCu₄, we measured the ¹⁵⁵Gd Mössbauer effect and neutron diffraction together with the magnetic susceptibility. It was concluded that the structure is partially disordered from the comprehensive analyses of the results.

2. Experimental procedures

Polycrystalline samples of GdInCu₄ were prepared by argon arc melting from 99.9%-pure Gd and 99.99%-pure In and Cu metals. No atomic disorder was detected by a Rietveld analysis of the x-ray diffraction pattern. The susceptibility was measured by a SQUID magnetometer (Quantum Design, MPMS-5). Mössbauer spectra were obtained by means of the 86.5 keV resonance of ¹⁵⁵Gd. Neutron-irradiated (¹⁵⁴Sm-enriched) SmPd₃ was used as a source material. The resonance spectra were analysed using a transmission integral formula with constrained source parameters and the natural linewidth $\Gamma_a = 0.25$ mm s⁻¹ for a GdInCu₄ absorber.

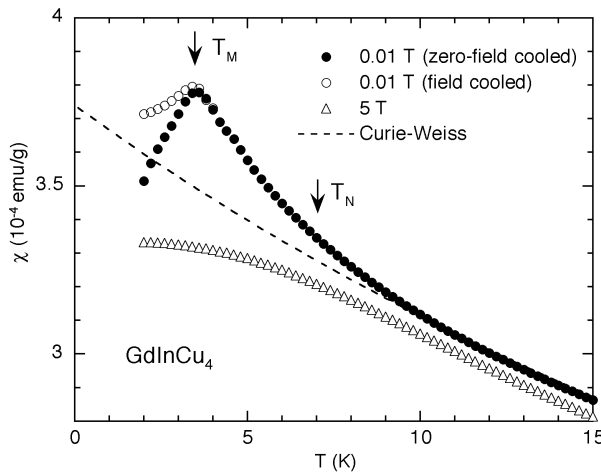


Figure 1. Temperature dependences of the magnetic susceptibility of GdInCu₄ measured at 0.01 T (●, ○) and 5 T (△). Under the field of 0.01 T, the susceptibility was measured under both zero-field-cooled (●) and field-cooled (○) conditions. The broken curve represents the Curie-Weiss behaviour extrapolated from high-temperature data.

Neutron diffraction was performed on the D4 diffractometer using a hot source ($\lambda = 0.499 \text{ \AA}$) at the Institut Laué–Langevin (ILL) in Grenoble.

3. Experimental results

3.1. Magnetic susceptibility

Some low-temperature parts of the magnetic susceptibility are shown in figure 1. Under a relatively low field of 0.01 T, a sharp peak was observed at around $T_M \simeq 3.5 \text{ K}$, which is about half of the value $T_N \simeq 7 \text{ K}$ determined from specific heat, electrical resistivity etc [5]. (It was confirmed that the same specimen shows a resistivity peak at another temperature of $T \simeq T_N$.) The susceptibility shows no distinct anomaly just at T_N , but deviates upward from the Curie–Weiss behaviour (the broken curve) below T_N . Interestingly, a field-cooling effect was found; the low-temperature susceptibility is increased by the field cooling but still shows a maximum at around T_M , suggesting anomalous glass-like freezing of the spins. It should also be noted that the specific heat shows a clear λ -type peak at T_N but does not exhibit a distinct anomaly at around T_M [5]. The low-temperature susceptibility is depressed and the sharp peak was smeared out by a large field (5 T), suggesting instability of the low-temperature state against field.

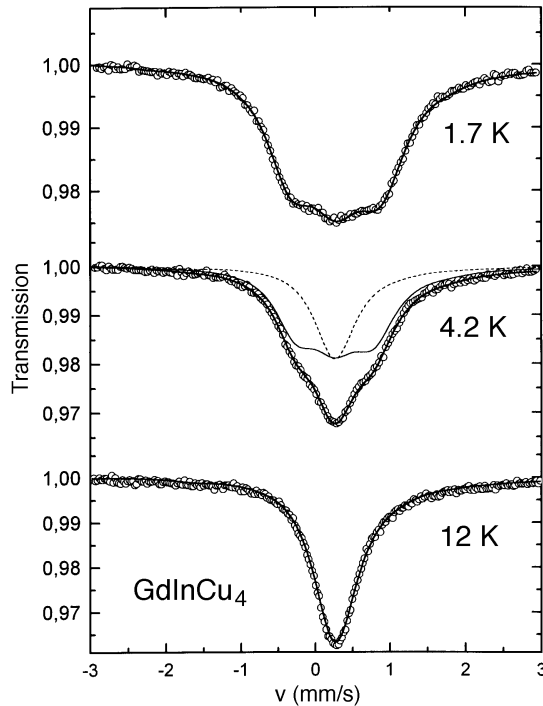


Figure 2. Typical examples of ^{155}Gd Mössbauer spectra for GdInCu_4 measured at 1.7, 4.2 and 12 K. The spectra at 12 and 1.7 K can be explained in terms of a single-line (paramagnetic) component and a Zeeman-split (antiferromagnetic) component, respectively. The spectrum at 4.2 K can be reproduced by assuming that a single-line component (---) and a Zeeman-split component (—) coexist.

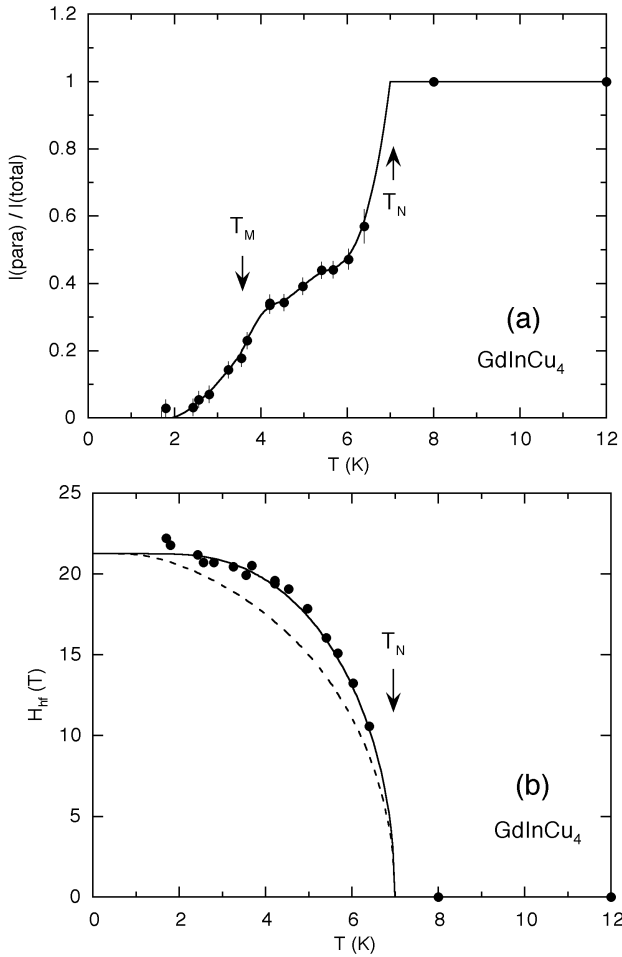


Figure 3. (a) The temperature dependence of the fraction of the paramagnetic component in the ^{155}Gd Mössbauer spectra for GdInCu_4 . The solid curve is a guide for the eye. (b) The temperature dependence of the hyperfine-field magnitude of the antiferromagnetic component. Solid and broken curves indicate the Brillouin functions for $S = \frac{1}{2}$ and $\frac{7}{2}$, respectively.

3.2. The ^{155}Gd Mössbauer effect

Figure 2 shows typical examples of ^{155}Gd Mössbauer spectra recorded at $T = 1.7\text{--}40$ K. At 12 K, a single-line spectrum was observed as expected for paramagnetic Gd^{3+} ions in a cubic site symmetry (i.e. with no quadrupolar interaction). By contrast, at 1.7 K, a magnetically split spectrum is apparent (although it is poorly resolved; this poor resolution is inherent to the ^{155}Gd Mössbauer effect), indicating that all of the Gd ions are in an ordered state. The saturation hyperfine field, H_{hf} , is estimated to be 22 T. At an intermediate temperature, 4.2 K, a single-line component and a Zeeman-split component seem to coexist. A least-squares fitting procedure based on the assumption of the coexistence of a paramagnetic component and a single magnetic component can reproduce the spectrum well, while a fit based on the assumption of a continuous distribution in the magnitude of the hyperfine field at the Gd site is less satisfactory; the R -factor of the latter fit amounts to 1.55 in comparison with 0.87 for

the fit with two components and, in addition, the two spectral components can be reproduced perfectly with the natural linewidth obtained from an independent experiment. This excludes the possibility of spatially inhomogeneous magnetic states such as a conventional spin glass and indicates that paramagnetic (dynamical) and antiferromagnetic (static) moments coexist even below T_N .

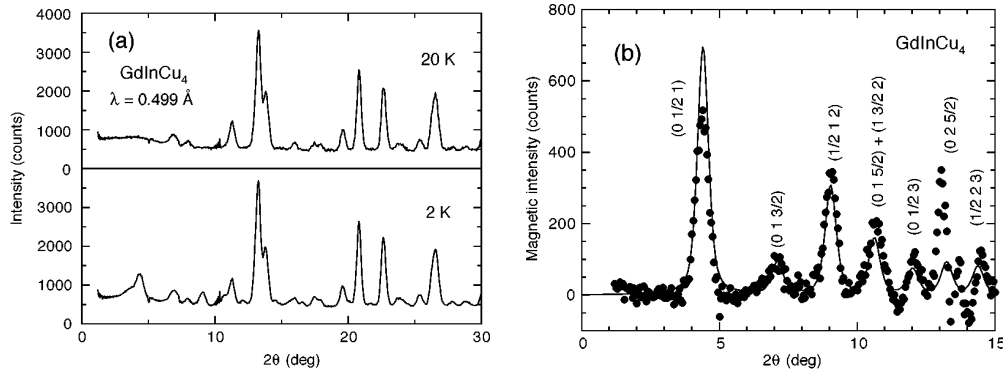


Figure 4. (a) Neutron diffraction patterns of $GdInCu_4$ measured at 20 and 2 K. (b) The magnetic diffraction pattern obtained by subtracting the intensity at 20 K from that at 2 K. The diffuse scattering was subtracted. The solid curve is the intensity calculated assuming a collinear type-III antiferromagnetic structure with spin directions parallel to [010].

Figure 3(a) shows the fraction of the paramagnetic component, which reduces to approximately a half just below T_N and decreases gradually at lower temperatures to become zero at 1.7 K. It is worth noting that the paramagnetic component decreases more quickly below 4 K, i.e. at a temperature slightly above the susceptibility peak at T_M . The temperature variation of H_{hf} for the antiferromagnetic component is also shown in figure 3(b). The fit with an $S = \frac{7}{2}$ Brillouin function (the broken curve) is not satisfactory, but a fit with an $S = \frac{1}{2}$ Brillouin function (the solid curve) reproduces the experimental result well (the best-fit parameter obtained, T_N , is 7.0 K). Although this good correspondence may be fortuitous, it is clear that the sublattice magnetization increases more quickly than is expected for a usual second-order phase transition of the $S = \frac{7}{2}$ system.

3.3. Neutron diffraction

A powder neutron diffraction measurement was performed using high-energy neutrons because of the considerable degree of absorption of thermal neutrons by the element Gd. We recorded powder diffraction diagrams at 20 and 2 K, which are shown in figure 4(a). Although the angular resolution is poor due to the high neutron energy, the diffraction peaks are sufficiently well articulated. All of the diffraction peaks at 20 K can be assigned to the nuclear Bragg peaks associated with the C15b structure, if one takes into account additional low-angle diffuse scattering (a broad hump centred at around $2\theta = 4^\circ$), which will be discussed below. At 2 K, additional peaks appear with no change in nuclear scattering. Figure 5(b) shows the magnetic scattering at 2 K, i.e. the difference profile for the patterns at 2 and 20 K. The diffuse scattering has been subtracted from this profile on the basis of a rather arbitrary assumption (see below). All of the observed magnetic peaks can be indexed as those of the fcc type-III antiferromagnetic structure ($Q = (0 \frac{1}{2} 1)$) as indicated in figure 4(b). Among the type-III collinear antiferromagnetic structures, the experimental intensity is in best agreement with the

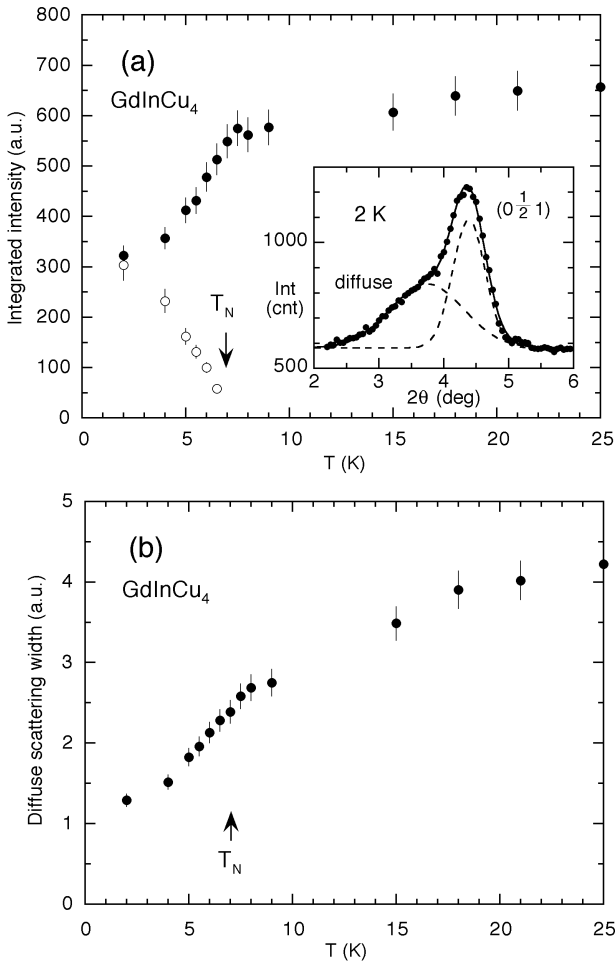


Figure 5. (a) Temperature dependences of the integrated intensity of the elastic $(0 \frac{1}{2} 1)$ peak (\circ) and the diffuse peak (\bullet) for GdInCu_4 . The inset shows a low-angle profile at 2 K. The solid curve is the least-squares fit to the data based on the superposition of two Gaussians (broken curves). (b) The temperature dependence of the width of the diffuse scattering.

one with spins parallel to [010]. However, as discussed below, the actual situation seems to be more complicated.

Another important feature of the neutron diffraction diagrams is the presence of diffuse scattering. A low-angle part of the diffraction profile at 2 K is magnified in the inset of figure 5(a). The complicated profile is interpreted as the superposition of the sharp $(0 \frac{1}{2} 1)$ Bragg peak and a broad diffuse scattering, whose maximum is located near the angle corresponding to the (001) peak (a main peak for the fcc type-I structure with $Q = (001)$). We followed the temperature variation of the low-angle profile for $T = 2\text{--}50$ K and analysed the results, tentatively, on the basis of the superposition of two Gaussians. As shown in figure 5(a), the intensity of the elastic $(0 \frac{1}{2} 1)$ peak decreases rapidly on approaching T_N . By contrast, the integrated intensity of the diffuse scattering increases rapidly up to T_N and becomes almost temperature independent above T_N . The characteristic width of the diffuse scattering shows

a temperature dependence similar to that shown in figure 5(b), indicating the reduction of the correlation length with increasing temperature. The diffuse scattering at sufficiently low temperatures is attributed to spin freezing with type-I-based short-range magnetic correlations, which coexist with the type-III long-range antiferromagnetic ordering. The diffuse scattering above T_N is attributed to the dynamical short-range magnetic correlations, which is consistent with the considerable lack of magnetic entropy above T_N [5]. Here it should be noted that the energy window in the present measurement is wider than those of usual diffraction experiments because the high-energy neutron source was used, implying that the diffuse scattering includes quasi-static (slowly dynamic) components with rather high energy.

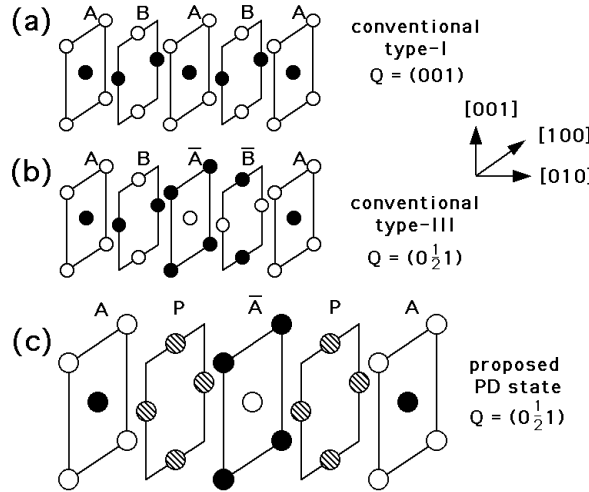


Figure 6. The conventional fcc type-I (a) and type-III (b) antiferromagnetic structures, where open and closed circles represent antiparallel spins. (c) indicates a possible magnetic structure of $GdInCu_4$ (a partially disordered state) just below T_N , where open and closed circles represent spins directed along $[010]$ and $[\bar{0}\bar{1}0]$, respectively, and hatched circles indicate paramagnetic (dynamical) spins, which are, however, assumed to have antiferromagnetic correlations within (010) planes.

4. Discussion

4.1. Possible magnetic structure: a partially disordered state

Neutron diffraction results suggest that type-III ($Q = (0 \frac{1}{2} 1)$) and type-I ($Q = (001)$) antiferromagnetic correlations compete in this fcc system. As shown in figures 6(a) and 6(b), the usual type-I and type-III structures are described as $\cdots ABAB \cdots$ and $\cdots A\bar{B}\bar{A} \cdots$ respectively, where A and B represent neighbouring (010) planes (with antiferromagnetic spin arrangements in the planes) and the bar denotes spin reversal. It should be noted that, if $J_2 = 0$, neighbouring planes do not interact at all and any stacking sequence gives the lowest exchange energy. In excited states, the fluctuation spectrum has a reduced dimensionality (two dimensions) [10], leading to weak coupling between (010) layers.

To explain both the Mössbauer and the neutron diffraction results, we propose the partially disordered structure shown in figure 6(c) as one of the possible magnetic structures just below T_N . Open and closed circles represent spins pointing along $[010]$ and $[\bar{0}\bar{1}0]$, respectively, and hatched circles indicate dynamical moments. This state is described as $\cdots PAP\bar{A} \cdots$ where P stands for a paramagnetic (dynamical) layer, although, in the P layers, we expect already

established antiferromagnetic correlations, i.e. dynamical fluctuations between B and \bar{B} states. This model leads to a 1:1 ratio of paramagnetic and antiferromagnetic moments, and exhibits the type-III modulation. The fractions among the magnetic Bragg intensities expected from this partially disordered structure are the same as those for the usual type-III structure with the same moment directions; however, the intensity of each peak is just half of the corresponding value for the conventional structure. The molecular fields produced by A and \bar{A} sublattices cancel at P.

With decreasing temperature, it is expected that the fluctuations in the P layers will gradually slow down and freeze as B or \bar{B} , leading to a glass-like transition of *layers*. The susceptibility peak at T_M may correspond to such a freezing; T_M is not a conventional phase transition temperature but a freezing point on the timescale of the susceptibility just like in the usual spin glass. This is in accordance with there being no anomaly in the specific heat at T_M and a fairly continuous variation in the fraction of the static component ‘seen’ by the neutron diffraction (figure 5(a)) and Mössbauer effect (figure 3(a)), which have timescales that are much faster and wider than those of the susceptibility. Depending on the frozen state of P, one may see local type-I arrangements. At finite temperature up to T_N , it is thought that the flipping of the antiferromagnetic layers or movement of the domain walls is thermally induced as excited states. Although it is not easy to explain the absence of a peak at T_N , such a behaviour has been observed for partially disordered states in frustrated triangular lattices [11, 12].

A quantitative analysis of the Gd ordered moment based on the neutron diffraction intensity also supports the above model. Assuming that only half of the Gd atoms in every second layer contribute to the sharp elastic Bragg peaks, we obtain $6.9 \pm 0.5 \mu_B/\text{Gd}$ (at 2 K), which is in good agreement with the saturation moment of Gd, $7 \mu_B$. The assumption that all Gd atoms participate in the type-III long-range ordering leads to an unphysical value of $4.9 \pm 0.4 \mu_B/\text{Gd}$. In other words, the moments of the other half of the Gd atoms do not form a long-range correlation, and hence they contribute to the diffuse scattering at the lowest temperature (see figure 5(b)).

The zero-field NMR spectra measured at 1.5 K reveal that local spin arrangements around In and Cu sites are simple and practically unique [13]. This is also consistent with the above model, since the *local* magnetic arrangements ‘seen’ from the In and Cu sites are unique and are the same for both type-I and type-III arrangements with spin directions parallel to [010].

4.2. The origin of the partially disordered state

Partially disordered states have already been found in some frustrated itinerant-electron systems (e.g. RMn_2 [14]) and in a few Kondo systems (e.g. CeSb [15] and UNi_4B [16]). In these cases, the local moments themselves are unstable and the paramagnetic phase is in a nonmagnetic state. However, GdInCu_4 does not belong to these categories, because Gd has a well-defined localized moment.

Among localized moment systems, partially disordered states have been found in triangular lattices with Ising-spin chains such as CsCoCl_3 [17] and CsCoBr_3 [18], in which both intra-chain and inter-chain interactions are negative (the former are very much dominant). In these compounds, one third of the chains remain paramagnetic below T_N down to $T_M \simeq T_N/2$. It is interesting to note that no anomaly was detected in the specific heat at T_M , where all of the spins become static [17, 18]. The case of GdInCu_4 is similar to this situation and may be the first example of a partially disordered phase which originates not from the moment instability but from the dynamical (entropy) effect in the fcc lattice. It seems, however, that no statistical model has so far predicted the occurrence of a partially disordered state in the fcc lattice [19], in contrast to the situation for the triangular lattice, for which a partially disordered state is

supported by theory [20]. Monte Carlo simulations for the Heisenberg fcc antiferromagnet have suggested a collinear type-I or type-III antiferromagnetic structure for small J_2 [21], probably due to the order by disorder [22], but not intimated a partially disordered state. Thus a partially disordered state is unlikely to appear in a simple classical or Heisenberg fcc lattice antiferromagnet. Some additional ingredients seem to be necessary.

Recently, Lacroix and co-workers [23] discussed the possibility of the partially disordered state in topologically frustrated systems from a general viewpoint by taking into account nn exchange energy of the Heisenberg type, the stability of the moment itself and uniaxial anisotropy. They concluded that the large magnetic anisotropy suppresses the creation of moments at certain sites and favours the partially disordered state. This theory was originally intended to explain the partially disordered state in itinerant and Kondo systems with unstable moments, but may be applied to localized moment systems at finite temperatures. Here, it is interesting to note the possible anisotropy in the exchange coupling between Gd moments via ligand atoms, which may originate in the characteristic electronic state in GdInCu_4 as a low-carrier-density system. In fact, anisotropic exchange was suggested by the anisotropic hyperfine field at the In site inferred from NMR experiments [13].

The low-carrier-density nature of the present system may be another factor that led to an anomalous spin structure. Magnetic polarons produced by low-density carriers could be responsible for the partially disordered state as proposed to explain the complex magnetic structures of Ce compounds [24].

The anomalous temperature dependence of the sublattice magnetization determined from H_{hf} (figure 3(b)) remains to be explained. Although theories have not explained the partially disordered state in the fcc lattice, first-order-like phase transitions or anomalous temperature dependences of the sublattice magnetization were predicted for the Ising lattice in a number of model calculations [25] and also for the Heisenberg lattice [21]. This may be interpreted as follows: spatial magnetic correlations, which are restricted to the two-dimensional planes in the frustrated state, recover to balance the magnetization in the ordered state, which is probably due to the order and disorder [22]. The slight upward deviation from the Curie–Weiss susceptibility below T_N may also be interpreted in the same context.

Finally, we have to comment on the effect of atomic disorder. Although we have detected neither chemical disorder from x-ray analyses nor sample dependence of the magnetic properties, we cannot exclude completely the possibility of a small degree of atomic disorder in the sense that a perfect specimen without defects is never obtained experimentally. This disorder may be related to the peculiar magnetic state in GdInCu_4 . However, even if this is the case, we believe that the partially disordered state is realized as a result of competing interactions due to the strong frustration on the fcc lattice.

5. Conclusions

Our work was aimed at determining the magnetic structure of the frustrated fcc antiferromagnet GdInCu_4 . As a possible magnetic structure, we propose a partially disordered state which exhibits type-III arrangements ($Q = (0\frac{1}{2}1)$). In this structure, only every second (010) layer exhibits long-range order. The remaining half of the Gd moments fluctuate dynamically even below T_N , and gradually slow down to freeze on approaching 0 K. We emphasize that this is the first example of a partially disordered state driven by the dynamical (entropy) effect in the localized moment fcc antiferromagnet.

Acknowledgments

The authors would like to thank H Fischer for his contribution to the neutron diffraction experiments, H Tanahashi for assistance in the SQUID measurements, M Mekata, Y Yamaguchi and N Metoki for helpful discussions and R Iehara for technical support. The Mössbauer effect measurements were supported by the State Committee for Scientific Research in Poland under Grant No 2 P302 033 05.

References

- [1] See, for example,
Chandra P and Coleman P 1995 *Strongly Interacting Fermions and High T_c Superconductivity* ed B Doucot and J Zinn-Justin (Amsterdam: North-Holland) p 495
- [2] Schiffer P and Ramirez A P 1996 *Comment. Condens. Matter Phys.* **18** 21
- [3] Anderson P W 1950 *Phys. Rev.* **79** 705
- [4] See, for example,
Smart J S 1966 *Effective Field Theories of Magnetism* (Philadelphia, PA: Saunders College)
- [5] Abe S, Atsumi Y, Kaneko T and Yoshida H 1992 *J. Magn. Magn. Mater.* **104–107** 1397
- [6] Nakamura H, Ito K, Wada H and Shiga M 1993 *Physica B* **186–188** 633
- [7] Nakamura H, Ito K and Shiga M 1994 *J. Phys.: Condens. Matter* **6** 6801
- [8] See, for example,
Reimers J N 1992 *Phys. Rev. B* **45** 7287
- [9] Moessner R and Chalker J T 1998 *Phys. Rev. Lett.* **80** 2929
- [10] Canals B and Lacroix C 1998 *Phys. Rev. Lett.* **80** 2933
- [11] See, for example,
Harris M J and Zinkin M P 1996 *Mod. Phys. Lett. B* **10** 417
- [12] Shiga M 1995 *Proc. 30th Zakopane School of Physics (Krakow)* (Singapore: World Scientific) p 57
- [13] Danielian A 1961 *Phys. Rev. Lett.* **6** 670
- [14] Danielian A 1964 *Phys. Rev.* **133** A1344
- [15] Alexander A and Pincus P 1980 *J. Phys. A: Math. Gen.* **13** 263
- [16] Hirakawa K, Ikeda H, Kadokawa H and Ubukoshi K 1983 *J. Phys. Soc. Japan* **52** 2882
- [17] Mekata M, Yaguchi N, Takagi T, Sugino T, Mitsuda S, Yoshizawa H, Hosooit N and Shinjo T 1993 *J. Phys. Soc. Japan* **62** 4474
- [18] Nakamura H, Kim N, Shiga M, Kmiec R and Tomala K 1999 *Proc. 11th Int. Conf. on Hyperfine Interactions (Durban); Hyperfine Interact.* at press
- [19] See, for example,
Shiga M 1994 *J. Magn. Magn. Mater.* **129** 17
- [20] Rossat-Mignod J, Burlet P, Villain J, Bartholin H, Wang Tcheng-Si, Florence D and Vogt O 1977 *Phys. Rev. B* **16** 440
- [21] Mentink S A M, Nieuwenhuys G J, Nakotte H, Menovsky A A, Drost A, Frikkee E and Mydosh J A 1995 *Phys. Rev. B* **51** 11567
- [22] Mekata M and Adachi K 1978 *J. Phys. Soc. Japan* **44** 806
- [23] Yelon W B, Cox D E and Eibschütz M 1975 *Phys. Rev. B* **12** 5007
- [24] See, for example,
Nakanishi K 1992 *J. Phys. Soc. Japan* **61** 2901
- [25] See, for example,
Mekata M 1977 *J. Phys. Soc. Japan* **42** 76
- [26] Takagi T and Mekata M 1995 *J. Phys. Soc. Japan* **64** 4609
- [27] Minor W and Giebultowicz T M 1988 *J. Physique Coll.* **49** C8 1551
- [28] Henley C L 1987 *J. Appl. Phys.* **61** 3962
- [29] See, for example,
Lacroix C, Canals B, Núñez-Regueiro M D, Coqblin B and Arispe J 1997 *Physica B* **230–232** 529
- [30] See, for example,
Kasuya T 1993 *J. Alloys Compounds* **192** 217
- [31] See, for example,
Phani M K, Lebowitz J L and Kalos M H 1980 *Phys. Rev. B* **21** 4027